Hindawi
Advances in Civil Engineering
Volume 2019, Article ID 6824543, 10 pages
https://doi.org/10.1155/2019/6824543

Research Article

Study of Shear Capacity of Jointed Rock Mass with Prestressed Anchor Bolt

Yufei Zhao,[1] **Hongtao Zhang**,[2] **and Yong Nie**[3]

[1]*Senior Engineer, State Key Laboratory of Simulation and Regulation of River Basin Water Cycle, China Institute of Water Resources and Hydropower Research (IWHR), Beijing 100038, China*
[2]*Associate Professor, College of Civil Engineering, North China University of Technology, Beijing 100144, China*
[3]*Ph.D. Candidate, State Key Laboratory of Simulation and Regulation of River Basin Water Cycle, China Institute of Water Resources and Hydropower Research (IWHR), Beijing 100038, China*

Correspondence should be addressed to Hongtao Zhang; zhanght@ncut.edu.cn

Received 21 September 2018; Accepted 4 February 2019; Published 20 June 2019

Guest Editor: Jian Sun

Rock mass failure caused by jointed plane is the common disaster in geotechnical engineering. Research on shearing property of jointed rock mass with prestressed anchor bolt and its mechanical property is an aspect for the stability analysis of rock slope and tunnel. This paper studies the stress and deformation of bolt and jointed plane, as well as anchored body and rock mass during shearing by indoor model testing and theoretical analysis. The shearing strength and mechanical property of anchored jointed plane have been systematically studied, and the additional force caused by deformation of prestressed anchor bolt and jointed rock mass during the shearing has been proposed and verified. The anchorage interaction between rock mass and bolt is revealed.

1. Preface

Rock mass is a composite medium which is sliced by various discontinuous jointed planes formed during the long-term geological tectonism, and its mechanical properties are highly complicated. Especially jointed planes scattered randomly within rock mass and the properties such as roughness, waviness, weak strength, and joint opening are strongly related to the shear strength of rock mass. Rock mass failure caused by large jointed plane is the most common disaster of practical geotechnical engineering. Reinforcement provided by rock bolt is the promotion of the natural self-supporting ability within the host rock mass. Mechanical properties of rock bolt and bolt failures caused by rock mass have been studied extensively in many ways, including laboratory and field tests [1–10], numerical simulations [11–17], and analytical method [18–23]. And, some scholars study its mechanical properties by analyzing its dynamic response recently [24–27].

The prestressed anchorage technique was first used in Algeria's Shelfa Dam in 1934, and its first application in China was the right dam foundation of Meishan reservoir in 1946. Thereafter, this technology has been widely used in geotechnical engineering. The scholars who first carried out physical model experiments on the mechanical properties of prestressed bolted rock mass are Ge and Liu [2] in China. They conducted indoor, in situ model tests and proposed a theoretical model which demonstrated that the reinforcement of anchored body was similar to pinned support and that prestressed anchor bolt could greatly improve the mechanical properties of jointed rock mass.

Prestressed anchorage can enhance the strength and stability of rock mass. In previous studies, little research has been done on the relationship of stress and deformation of prestressed anchored body and the coupling effect of anchor bolt and jointed plane. The deformation of anchored jointed plane and anchor bolt during shearing and the distribution of stress and strain within bolt are not fully understood yet.

This paper considers the jointed plane as indented structure and compares the different effect between prestressed anchored body and non-prestressed one. The shearing deformation of bolt and the plastic distribution is

studied, as well as the bolt deformation and normal displacement of jointed plane. Meanwhile, indoor model testing is conducted to analyze the shear property of the bolt related with deformation during shearing. Finally, combined with mechanical analysis of anchor body, the shear capacity of jointed rock mass and the interaction is developed and verified.

2. Mechanical Properties of Jointed Plane

In actual projects, the jointed planes scattered within rock mass are not always parallel, and most times, the two surfaces of jointed plane are full of irregular convex pieces with great discontinuity and undulation, resulting in significant differences of mechanical properties according to their shape.

The shear strength of irregular rigid jointed plane needs to be studied firstly. The most representative one is the double linear model proposed by Patton [28]. Based on Patton's shear strength equation of irregular indented jointed plane under lower normal stress level, the critical normal stress of jointed plane climbing under different normal stress is proposed:

$$\sigma_m = \frac{c_r - \left(c_j / \left(2 \times \left(\cos i - \sin i \times \tan \varphi_j\right) \times \cos i\right)\right)}{\tan\left(\varphi_j + i\right) - \tan \varphi_r}, \quad (1)$$

where σ_m (MPa) is the critical normal stress under the condition that no climbing failure occurs on the jointed plane; φ_r is the rock internal friction angle; c_r (MPa) is the rock cohesion; φ_j is the jointed plane friction angle; c_j (MPa) is the jointed plane cohesion; and i is the climbing angle of indented jointed plane. All these related variables are shown in Figure 1.

Therefore, under different normal stress level, indented jointed plane shows different shear failure strength during the climbing period:

$$\begin{cases} \tau = \sigma \cdot \tan\left(\varphi_r + i\right) + \dfrac{c_j}{2 \times \left(\cos i - \sin i \times \tan \varphi_j\right) \times \cos i}, & \sigma < \sigma_m, \\ \tau = \sigma \cdot \tan \varphi_r + c_r, & \sigma \geq \sigma_m. \end{cases} \quad (2)$$

In the backslide period, the shear strength of regular indented jointed plane is

$$\tau = \sigma \cdot \tan\left(\varphi_r - i\right). \quad (3)$$

The shear testing curve of indented rock jointed plane is shown in Figure 1, where the shear stress on jointed plane shows a roughly linear correlation with its shear strain during the climbing period, but after reaching the peak value, with the increase of shear strain, shear stress decreases. In Figure 1(a), the three lines, respectively, represent the theoretical relationship between shear stress and normal stress of climbing period, rock cutting period, and backslide period. The schematic diagrams of three different rock shearing periods are shown in Figure 1(b).

In reinforcement slope, the normal stress of jointed plane in the potential sliding zone ranges from 0 to 4 MPa which is relatively low, which means equation (2) has applicability in estimating the shear strength of irregular jointed plane in lower stress level. By average projection angle of instable limestone slope in bedding surface trace, Patton pointed out that the rougher the surface of the layer, the bigger the slope angle; at the same time, the average trace angle approximately equals the sum of the average surface projection angle and the basic friction angle of the flat jointed plane from the experiment.

After getting bolted, the jointed plane strength can be greatly promoted and its mechanical properties will become more sophisticated. Thus, indoor model testing combined with theoretical analysis is necessary to study the bolted jointed plane, in order to determine the contribution and influence of the prestressed bolt for the shear strength of jointed plane.

3. Indoor Model Test

3.1. Scheme of Model Test. In order to analyze the correlation between shear strength of bolted jointed plane and its shear displacement, indoor model testing is designed to conduct shearing test under different normal stress conditions. Mechanical parameters of the material used in model testing are listed in Table 1.

Concrete specimen with indented structural plane is manufactured in mold with the size of 300 × 300 × 150 mm (length × width × height), and the initial dilatation angle of structural plane is 33° manmade. After finishing sample solidification, two concrete specimens are placed upon each other and a hole is punched in the center where bolt is placed and cement grout infused; then, two ends of the bolt are locked and the angle between anchorage and jointed plane is 90°. The schematic diagram of testing specimen is shown in Figure 2. The bolt used in the experiment is Ø8 aluminum alloy bar with the length of 200 mm. Figure 3 shows the model test sample and the test equipment.

The specimen is set up on direct shear apparatus, and the shear test is conducted with shear rate of 0.5 mm/min under the normal stress of 0.2 MPa, 0.35 MPa, and 0.7 MPa, respectively. The experimental steps are based on the Chinese Standard Specifications for rock tests in water conservancy and hydroelectric engineering, *SL264-2001*.

According to the test, under the action of shear load, the shear strength of the anchorage mainly comes from three aspects: the shear characteristics of rock itself, the resistance of axial force, and the pinned action of anchor bolt. In order to study the influence degree of factors in the shear process,

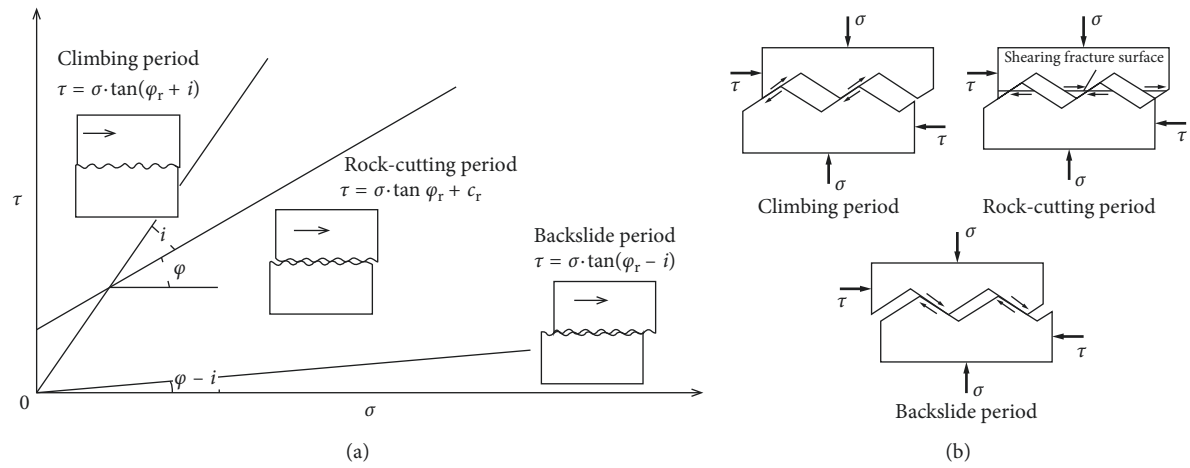

Figure 1: The shear stress and normal stress of indented rock structural plane in different periods.

Table 1: Mechanical parameters used in model testing.

	Density (kN/m^3)	Mechanical parameters					
		Friction coefficient	Cohesion (MPa)	Elastic modulus (GPa)	Poisson ratio	Yield strength (MPa)	Yield strain
Rock mass	2600	1.2	2.0	26.7	0.19	—	—
Plane	—	0.55	0	—	—	—	—
Bolt	2700	—	—	70.0	0.33	450	0.02
Grout	2600	0.87	1.0	19.0	0.23	—	—

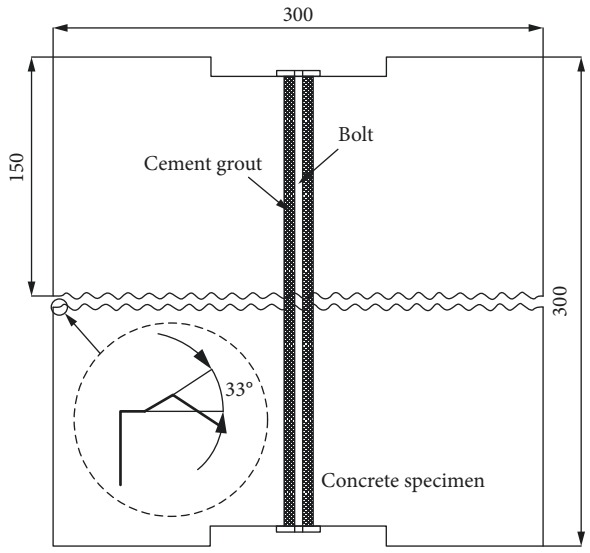

Figure 2: The schematic diagram of testing model (unit: mm).

the shear contrast tests of three anchoring are shown in Figure 4, which are no anchor bolt, anchor bolt with one end fixed and another end free, and anchor bolt whose prestress is 2.5 kN.

3.2. Model Test Result. The different conditions' influence on shearing characteristics of regular indented jointed plane and its shear strength are studied. The deformation feature and axial force change of prestressed bolt with the development of shear displacement is also examined.

3.2.1. Failure Mode of Jointed Rock Mass. Indoor model testing demonstrates that the failure status of prestressed bolted specimen of regular indented plane is highly related to its normal stress level.

While under lower normal stress level, shear displacement with remarkable crack may occur in rock mass, and the failure status displayed by the experiment is the significant extrusion and fracturing of rock mass by anchorage material.

While under higher normal stress level, the sample failure is approximately in accordance with the one of nonbolted joint rock masses under same normal stress.

3.2.2. Shear Strength. Through direct shear testing of prestressed bolted regular indented jointed plane, it can be inferred that, when compared with the experiment result of nonprestressed bolted joint rock mass, its shear strength is greatly improved, and if higher prestress is imposed in bolt, its shear strength could be further improved.

Figure 5 shows the shear strength-shear displacement curves of the structural plane under 3 groups of different normal stress conditions (0.7 MPa, 0.35 MPa, and 0.2 MPa). Each group of tests included shear tests under three different anchorage conditions. It can be intuitively seen from Figure 5 that the anchorage condition has a considerable impact on the shear strength of the structural plane.

In order to further analyze the shear behavior of anchored structural plane, the shear resistance under different anchorage conditions is analyzed and sorted out, which is shown in Table 2.

(a) (b)

Figure 3: The model test sample and the test equipment.

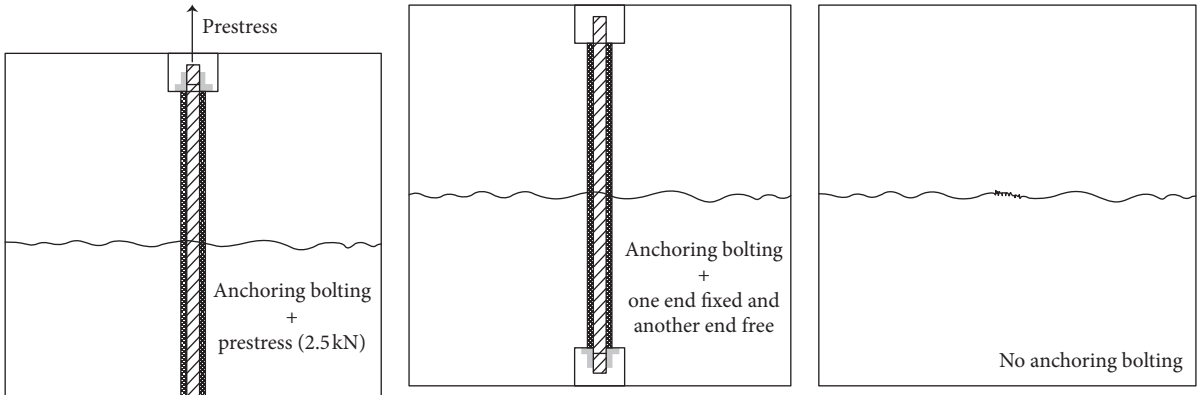

Figure 4: Schematic diagram of three anchorage modes.

It is obvious that the magnitude of prestress has a significant influence on the initial shear stiffness. Compared with the prestressed anchorage samples with normal stress of 0.2 MPa, when the normal stresses were 0.7 MPa and 0.35 MPa, the initial shear strength of the prestressed anchorage sample were increased by 150% and 52%, respectively. For one end-free samples, the increases of initial shear strength were 178% and 44%, respectively, and the initial shear strength of the no anchoring bolting samples were increased by 214% and 53%, respectively.

As can be seen from Table 2, when the normal stresses of 0.7 MPa, 0.35 MPa, and 0.2 MPa, the initial shear strength of the prestressed anchorage sample was increased by 10%, 37%, and 38%, respectively, and the initial shear strength of the one end-free sample was increased by 8%, 15%, and 22%, respectively, compared with that of the no anchoring bolting samples.

From the above, the increase of shear resistance of the initial stage in the shear test has an important relationship with the normal stress and prestress.

4. Theoretical Analysis

Indoor physical model testing indicates that for rigid jointed plane after prestressed bolt, dilatation effect will occur during shearing because of the undulation of jointed plane. The anchorage cable will deform like "S" shape in common rigid jointed plane. With the development of shear displacement, the anchorage cable within limited zone begins to deform, and with this deformation, its shear effect begins to work. The characteristics of jointed plane during shearing will be examined through theoretical and mechanical analysis in different phases. And, the failure mode will be determined by material parameters derived from model testing.

4.1. Mechanical Properties of Prestressed Bolt. The prestressed bolt deforms gradually with the development of jointed plane's shear displacement, but the deformation zone of bolt is somehow limited. This phenomenon is primarily related to the material properties of the bolt and jointed plane. We can call the major deformation zone of bolt as effective length since the deformation of prestressed bolt is concentrated within limited effective length. But, under shear load, the stress fluctuation length of bolt is longer than the effective length defined above. It can be seen from Figure 6 that the length with displacement or deformation is about twice the effective length, and this conclusion is supported by other studies also.

In Figure 6, P_u is the bearing capacity of grouting body or rock mass. It can be seen that bending moment at point D is

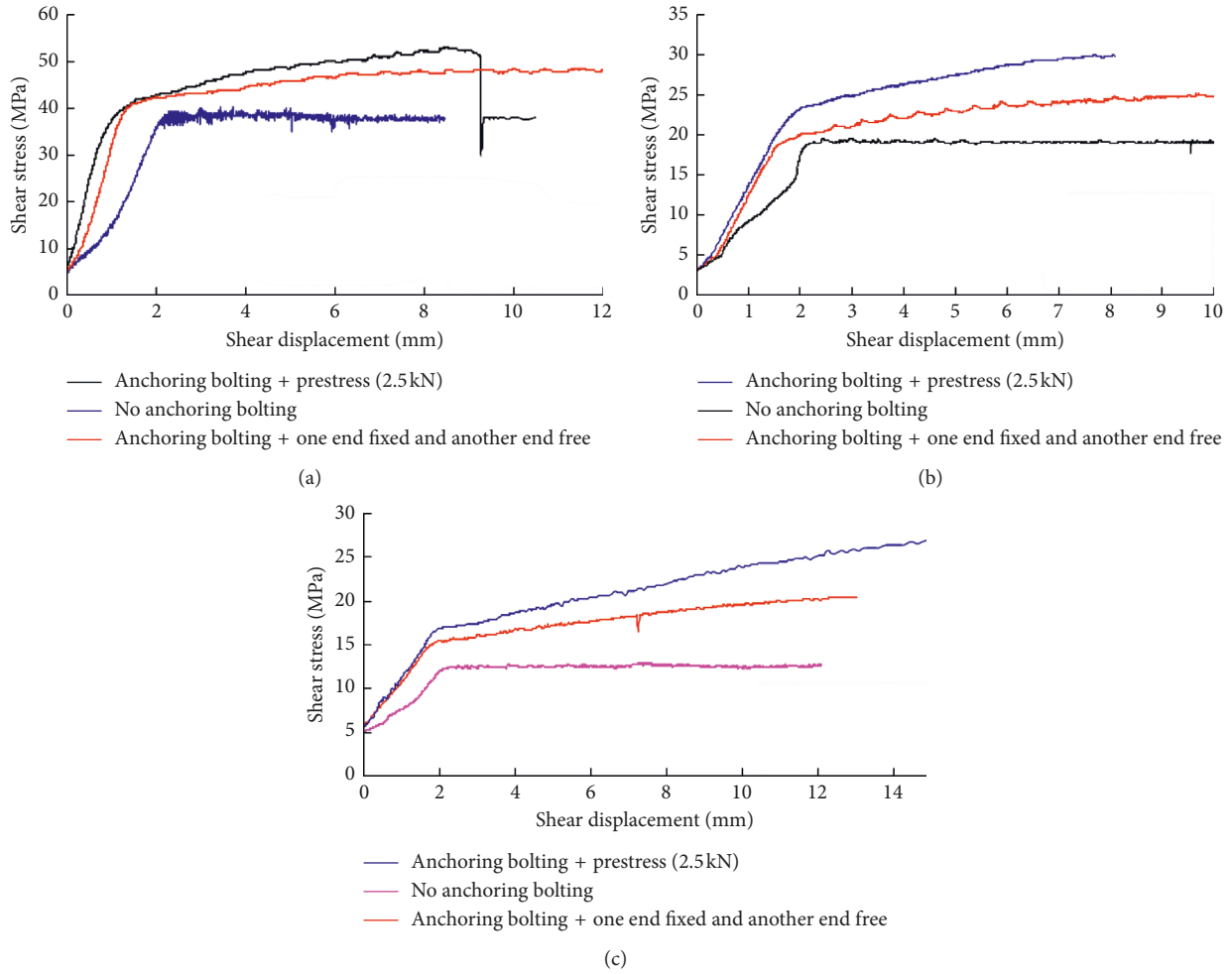

Figure 5: Shear stress-shear displacement curves with different anchorage conditions. (a) Normal stress 0.7 MPa. (b) Normal stress 0.35 MPa. (c) Normal stress 0.2 MPa.

Table 2: Initial shear strength in shear test under different anchorage conditions.

Normal stress (MPa)	Shear strength of the jointed surface at the initial shear stage* (kN)		
	Anchoring bolting + prestress** (2.5 kN)	Anchoring bolting + one end fixed and another end free	No anchoring bolting
0.70	42.80	41.98	39.00
0.35	25.95	21.71	18.95
0.20	17.12	15.11	12.42

*Shear strength at the initial shear stage is the shear strength corresponding to the turning point in the shear curve in Figure 5. **The force of 2.5 kN is the prestress applied when the anchor rope is locked. In other words, the force of 2.5 kN is the prestress of anchor cable before the normal stress is applied to the rock mass.

largest and accordingly internal tension is largest. If major force length is defined as twice the effective length of bolt deformation, when prestressed bolt is anchored perpendicular to jointed plane, with shear load caused by the development of shear displacement, the major force length of bolt can be formulated as follows:

$$2L_p = 2.31D_b\sqrt{\frac{\sigma_y}{P_u}\left[1-\left(\frac{T_0}{T_y}\right)^2\right]}, \quad (4)$$

where D_b is the diameter of bolt, σ_y is the yield stress of bolt, P_u is the bearing capacity of grouting body or rock mass, T_y is the yield force of bolt, and T_0 is the initial prestress in bolt.

When considering the angle between anchorage bolt and jointed plane, the major force length can be expressed as follows:

$$2L_p = \frac{2.31D_b}{\sin\alpha}\sqrt{\frac{\sigma_y}{P_u}\left[1-\left(\frac{T_0}{T_y}\right)^2\right]}, \quad (5)$$

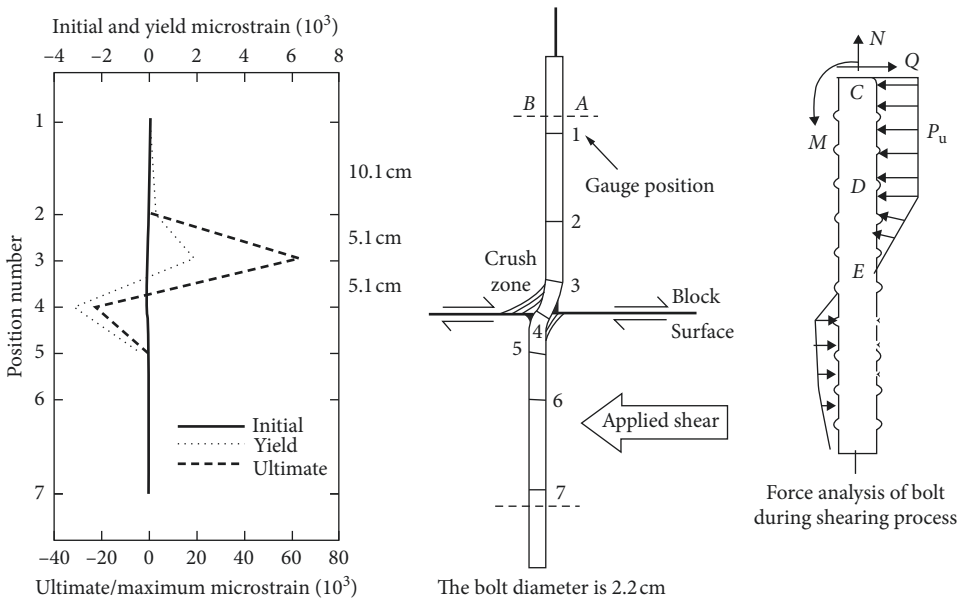

Figure 6: Diagram on deformation analysis of the bolt during the shearing process [29].

where α is the angle between anchorage bolt and jointed plane.

The derivation of formulas (4) and (5) is shown in Appendix.

With the development of shear displacement, the anchorage bolt gradually reaches its yield limit. According to different characteristics of jointed plane, rock fragment strength and material characteristics of bolt, the yield failure of bolt during shearing process of jointed plane are basically divided into the following two kinds:

(i) If the stiffness of the lateral walls of jointed plane or cement grout is relatively large, the prestressed bolt in jointed plane will probably produce tensile shear yield damage.

(ii) If the stiffness of the lateral walls of jointed plane or cement grout is relatively small, the prestressed bolt in the jointed plane will produce bending yield under bending effect, and two symmetric plastic hinges will be formed on both sides of jointed plane. After that, shear displacement will further develop and the extrusion destruction of bolt stops to grow into its deeper part.

According to the Von-Mises discipline of metallic materials' plasticity, when shear yield occurs, the stress condition of bolt's middle point is

$$\sqrt{\sigma^2 + 3\tau^2} = \sigma_y, \tag{6}$$

where σ_y is the yield strength stress of bolt material. When the prestressed force in bolt, $\sigma = (N_a + N_r)/A$, and N_a is the axial force in bolt during the shear process and N_r is the prestressed axial force in bolt.

When bending yield of bolt finally occurs, under the combination of moment and axial force upon bolt, the maximum normal stress will be defined as follows:

$$\sigma_A = \frac{M_0}{W} + \frac{N_0}{A} = 1.7\sigma_y. \tag{7}$$

The differential equation is constructed upon the basis of the mechanical analysis of anchorage body, and combined with the analysis of yield mode of the anchorage body, interactive solution could be derived.

4.2. Anchorage Interaction between Bolt and Rock. Reinforcing jointed plane with the prestressed bolt is mainly to impose constraints along its normal direction and shear direction when the structural plane is under external load.

The normal constraint primarily comes from the prestress of bolt, and normal constraint is imposed to structural plane through anchor pier (anchor plate) and the friction between bolt and hole wall. The shear constraint comes from two major factors: one is the friction between layers and fractures increased by normal constraints and the other is shear stress provided by bolt material itself.

When jointed plane is under shear load, the anchorage's contribution for jointed plane's shear resistance is reflected in the following three aspects.

4.2.1. Prestress. If the installation angle of the bolt is not completely perpendicular to jointed plane, the initial prestress of bolt has two components: one is the component perpendicular to jointed plane and the other is the parallel one.

Considering the bending deformation of bolt during shearing, the angle of bolt needs to be modified; and within the two components of initial stress, the expressions of component perpendicular to jointed plane $R_{T\sigma}$ and the parallel one $R_{T\tau}$ are as follows:

$$R_{T\sigma} = T_0 \sin(\gamma),$$
$$R_{T\tau} = T_0 \cos(\gamma), \tag{8}$$

where γ is the angle after bolt deformation.

4.2.2. Axial Force. Under shear load, the relative movement between interface of jointed plane causes the axial deformation of bolt related to axial force N and the normal displacement of jointed plane's dilatation related to additional axial force which has two components perpendicular and parallel to jointed plane and can be deduced by following method.

Under shear load, the bending and extension deformation of bolt is caused by the relative displacement of interface of jointed plane and the dilatation accordingly; and the additional axial force of bolt increases as well. The axial strain of bolt happens primarily within the major stress length, as shown in Figure 7.

The expression of additional axial force is as follows:

$$R_\Delta = \frac{\pi D^2 E_b}{4}\left(\frac{2L\sin\alpha + m\delta\tan i}{2L\sin\gamma} - 1\right),$$
$$\gamma = \arctan\left(\frac{2L\sin\alpha + m\delta\tan i}{2L\cos\alpha + m\delta}\right), \tag{9}$$

where $2L$ is the effective force length, α is the angle between anchorage bolt and jointed plane, i is the dilatancy angle, E_b is the elastic modulus of bolt; and m is the mobilization factor. The effective force length is the main part of the area of bolt deformation, and the gradually damping area of the bolt deformation is the 0.8 times of the area of bolt deformation.

Except for shear displacement, the axial force is mostly related to major stress length, bolt's elasticity modulus, the dilatation angle, and the diameter of bolt. And, the major stress length is related to the rock mass strength and the magnitude of prestress force.

Additional axial force can be disposed into two components: one is the component $R_{\Delta\sigma}$ perpendicular to jointed plane and the other is the parallel $R_{\Delta\tau}$, as shown in the following equation:

$$R_{\Delta\sigma} = \frac{\pi D^2 E_b}{4}\left(\frac{2L\sin\alpha + m\delta\tan i}{2L\sin\gamma} - 1\right)\sin\gamma,$$
$$R_{\Delta\tau} = \frac{\pi D^2 E_b}{4}\left(\frac{2L\sin\alpha + m\delta\tan i}{2L\sin\gamma} - 1\right)\cos\gamma. \tag{10}$$

Before the formation of plastic hinge, the stress of bolt is largely concentrated within major stress length. After the formation of plastic hinge, deformation and stress are primarily concentrated within the effective length between two plastic hinges. Because the anchorage body has already been in plastic stage, the increase of axial force slows down with the diminishment of bolt rigidity.

4.2.3. Shear Force. The anchorage body constrains the jointed plane's relative moment by its own shear force. The axial force of the bolt after certain deformation also has two components: one is parallel to jointed plane and the other perpendicular to it. The parallel component is pinned support resistance R_d, which can be deduced by the following method.

When plastic hinge forms, the pinned resistance of anchorage body can be expressed as follows:

$$R_d = \frac{D_b^2}{4}\sqrt{1.7\pi\sigma_y P_u\left[1 - \left(\frac{T_0}{T_y}\right)^2\right]}, \tag{11}$$

where D_b is the diameter of bolt, σ_y is the yield stress of bolt, P_u is the bearing capacity of grouting body or rock mass, T_y is the yield force of bolt, and T_0 is the initial prestress in bolt.

Before plastic hinge occurs, the pinned resistance is deduced with the force balance formula:

$$R_d = P_u D_b L, \tag{12}$$

where L is equal to the half of the force length of bolt. According to balance equation and yield criterion, the primary stress length of anchorage body can be identified; then the pin resistance can be determined according to different phases.

The pin resistance is not only related to shear displacement but also closely decided by rock mass strength, prestress level, and bolt diameter. According to bolt tilt after displacement, the pin resistance can also be decomposed to the component parallel to jointed plane and the perpendicular one, as follows:

$$R_{d\tau} = R_d \sin(\gamma),$$
$$R_{d\sigma} = -R_d \cos(\gamma). \tag{13}$$

Equation (13) shows that when bolt tilt is acute, the function of the perpendicular component of pin shear is negative; and the smaller the angle, the more negative its value.

5. Comparison between Theoretical Analysis and Experiment

Combined with the basic situation of the samples in the laboratory model test, the numerical model is established. The size of the model is 30 cm ∗ 30 cm ∗ 30 cm, the size of the upper model is 30 cm ∗ 30 cm ∗ 15 cm, and the size of the lower model is 30 cm ∗ 30 cm ∗ 15 cm. In the model, the size of initial dilatation angle is 5 mm in height, 15 mm in width, and the climbing angle is 33°.

In the numerical simulation, normal stress is applied by the direct shear test method, and the shear load is applied by the displacement control method. The rate of load application is 0.5 mm/min. Table 3 is a list of numerical simulation parameters.

Combined with experiment results and theoretical formulas, this sector will analyze the contribution of various mechanical effects to the shear resistance of bolted rock mass structural plane.

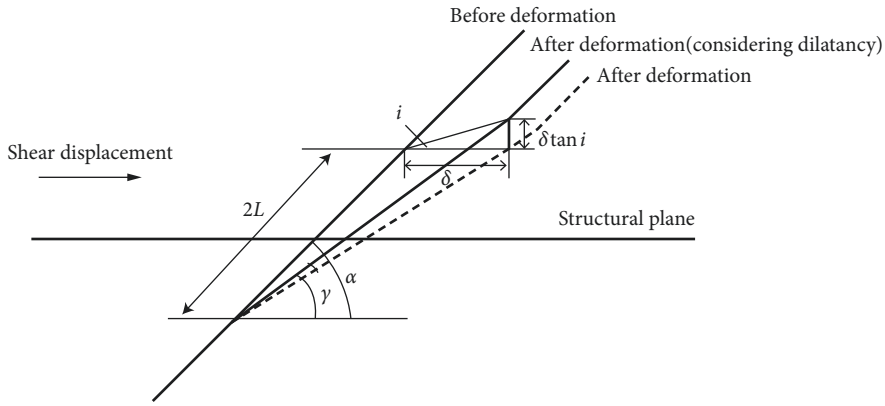

Figure 7: The bending and deformation of bolt.

Table 3: Numerical simulation parameters.

	Volume weight (kN/m^3)	Shear strength parameters		Deformation parameters		
		Frictional coefficient	Cohesive force (MPa)	Elasticity modulus (GPa)	Poisson's ratio	Yield strength (MPa)
Rock mass	2600.0	1.2	2.0		0.2	—
Structural plane	—	0.6	—	—	—	—
Anchor cable	2700.0	—	—	69.0	0.3	450.0
Grouting material	2600.0	0.9	1.0	19.0	0.2	—

The strength of rock samples is random. In order to conduct more accurate comparative analysis, only the samples with broken aluminum bar after shearing are selected. The test conditions are normal stress 0.2 MPa (that is, prestress 2.7 kN), normal stress 0.35 MPa (that is, prestress 6.6 kN), and normal stress 0.7 MPa (that is, prestress 1.2 kN).

The shear mechanical effects under three test conditions at the end of the initial stage are shown in Table 4. The axial force here is the sum of prestress and axial force caused by additional deformation.

Table 4 demonstrates that the theoretical calculation of pinned support is in good accordance with the testing measurements. Although bolt is lubricated beforehand, the friction between bolt and cement grout is inevitable; thus the tested pinned resistance includes part of axial force and is generally larger than actual value.

From experiment, for bolted smooth structural plane at the initial stage, with the increase of normal stress, the contribution of pinned resistance increases gradually and the contribution of axial force diminishes accordingly.

6. Conclusion

Based on the verification of theoretical analysis and physical model testing, the mechanical characteristics of bolted jointed rock mass during shearing can be summarized as follows:

(1) Under different normal stress levels, the failure patterns of undulant jointed plane are different. With the increase of normal stress level, undulant climbing effect diminishes gradually and finally grows to rock cutting damage. Besides, with the increase of normal stress, the normal displacement caused by jointed plane climbing angle decreases accordingly. From the monitoring points of normal displacement, it can be inferred that, along shear direction, the difference of normal displacement between the front and back sides of jointed plane is significant, which fully demonstrates the sliding resistance and shear effect of the anchorage cable.

(2) After anchored, the bolt deforms as "S" shape during shearing process; and the prestressed bolt is divorced from cement grout within certain range and loses effectiveness correspondingly.

(3) The study on stress distribution pattern of bolted rock mass during shearing demonstrates that, with the increase of shear displacement, the axial force of stretched bolt causes a compressive stress zone on rock mass through anchor pier. This compressive stress heightens jointed plane's normal stress level and improves its shear strength during shearing.

(4) After the bolt in anchored, the jointed plane is prestressed, and a spindle shape compressive stress zone appears in rock mass; model experiment indicates that the prestressed bolt also contribute to the timely supporting of rock mass when shear displacement of jointed plane develops.

(5) It can be concluded that the prestress of bolt contributes restrictedly to the improvement of bolted jointed plane's shear strength, and the main effect of anchorage in jointed plane is improving its sliding resistance and shear by bolt deformation during shearing.

Table 4: The shear strength with different normal stress conditions.

Normal stress (MPa)	Method	Shear strength increased (kN)	Axial force		Pin resistance	
			Force (kN)	Proportion (%)	Force (kN)	Proportion (%)
0.2	Model test	4.70	2.01	42.70	2.69	57.30
	Theoretical	5.60	3.08	55.00	2.52	45.00
0.35	Model test	7.00	4.24	60.50	2.76	39.50
	Theoretical	7.73	5.04	65.20	2.69	34.80
0.7	Model test	3.80	0.82	21.60	2.98	78.40
	Theoretical	4.67	1.38	29.60	3.29	70.30

In this paper, the research is mainly confined to a single bolt's effect during jointed plane's shearing process. The sliding resistance and shear of group anchors during jointed plane's shearing need to be identified in further studies. And, the various patterns of bolt deformation and stress distribution at different places of bolt along its shear and normal direction need to be considered in order to provide enough technical support and important references for the reinforcement design of jointed rock mass in projects.

Appendix

Under a load of axial force and bending moment, the plasticity yield of metal satisfies

$$\left(\frac{T}{T_y}\right)^2 + \frac{M}{M_y} = 1, \tag{A.1}$$

where T is the axial stress of bolt, T_y is the tensile yield stress of bolt, M is the bending moment, and M_y is the edge yield bending moment of bolt, where $M_y = 1.7\sigma_y((D_b^3\pi)/32)$.

Substitute M_y into formula (A.1), then

$$\left(\frac{T_D}{T_y}\right)^2 + \frac{M_D}{1.7\sigma_y((D_b^3\pi)/32)} = 1, \tag{A.2}$$

where D_b is the diameter of the bolt and σ_y is the yield stress of bolt.

In Figure 8, if the bending moment at point D is the largest, then the shear force at point D is 0. According to the balance of the force at the CD segment of the bolt, then there is

$$Q_C - P_u D_b L_p = 0, \tag{A.3}$$

$$M_D = \frac{1}{2}P_u D_b L^2. \tag{A.4}$$

Combining formulas (A.3) and (A.4), we get

$$Q_C = \frac{D_b^2}{4}\sqrt{1.7\pi\sigma_y P_u\left[1-\left(\frac{T_D}{T_y}\right)^2\right]}, \qquad P_u L^2 = \left[1-\left(\frac{T_D}{T_y}\right)^2\right]\frac{1.7\pi D_b^2\sigma_y}{16}. \tag{A.5}$$

Then, the effective length of the full-length bolt is

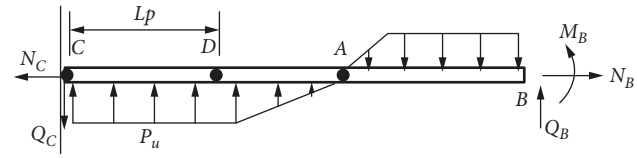

Figure 8: Deformation analysis of bolt.

$$2L = 2D_b\sqrt{\frac{1.7\pi\sigma_y}{16P_u}\left[1-\left(\frac{T_0}{T_y}\right)^2\right]} = 1.155D_b\sqrt{\frac{\sigma_y}{P_u}\left[1-\left(\frac{T_0}{T_y}\right)^2\right]}, \tag{A.6}$$

where P_u is the bearing capacity of grouting or rock mass and T_0 is the initial prestress.

Then, the major force length is

$$2L_p = 2.31D_b\sqrt{\frac{\sigma_y}{P_u}\left[1-\left(\frac{T_0}{T_y}\right)^2\right]}. \tag{A.7}$$

When considering the angle between anchorage bolt and jointed plane, the major force length can be expressed as

$$2L_p = \frac{2.31D_b}{\sin\alpha}\sqrt{\frac{\sigma_y}{P_u}\left[1-\left(\frac{T_0}{T_y}\right)^2\right]}, \tag{A.8}$$

where α is the angle between the anchorage bolt and jointed plane.

Data Availability

The experimental data used to support the findings of this study are available from the corresponding author upon request.

Conflicts of Interest

The authors declare that they have no conflicts of interest.

Acknowledgments

This research was supported by the National Key R&D Program of China under project no. 2018YFC0407003, Natural Science Foundation of China with grant no. 51409283, and the State Key Laboratory of Simulation and Regulation of River Basin Water Cycle.

References

[1] X. Feng, N. Zhang, S. Yang, and F. He, "Mechanical response of fully bonded bolts under cyclic load," *International Journal of Rock Mechanics and Mining Sciences*, vol. 109, pp. 138–154, 2018.

[2] X. Ge and J. Liu, "Study on the shear resistance behaviour of bolted rock joints," *Chinese Journal of Geotechnical Engineering*, vol. 10, no. 1, pp. 8–19, 1988.

[3] G. Grasselli, "3D behaviour of bolted rock joints: experimental and numerical study," *International Journal of Rock Mechanics and Mining Sciences*, vol. 42, no. 1, pp. 13–24, 2005.

[4] H. Jalalifar and N. Aziz, "Experimental and 3D numerical simulation of reinforced shear joints," *Rock Mechanics and Rock Engineering*, vol. 43, no. 1, pp. 95–103, 2010.

[5] Y. Li, H. Zhou, L. Zhang, W. Zhu, S. Li, and J. Liu, "Experimental and numerical investigations on mechanical property and reinforcement effect of bolted jointed rock mass," *Construction and Building Materials*, vol. 126, pp. 843–856, 2016.

[6] R. Pan, Q. Wang, B. Jiang et al., "Failure of bolt support and experimental study on the parameters of bolt-grouting for supporting the roadways in deep coal seam," *Engineering Failure Analysis*, vol. 80, pp. 218–233, 2017.

[7] M. Salcher and R. Bertuzzi, "Results of pull tests of rock bolts and cable bolts in Sydney sandstone and shale," *Tunnelling and Underground Space Technology*, vol. 74, pp. 60–70, 2018.

[8] B. Wang, X. Guo, F. Li, D. Hu, and Y. Jia, "Mechanical behavior of rock bolts under a high temperature environment," *International Journal of Rock Mechanics and Mining Sciences*, vol. 104, pp. 126–130, 2018.

[9] S. Yazici and P. K. Kaiser, "Bond strength of grouted cable bolts," *International Journal of Rock Mechanics and Mining Sciences & Geomechanics Abstracts*, vol. 29, no. 3, pp. 279–292, 1992.

[10] B. Zhang, S. Li, K. Xia et al., "Reinforcement of rock mass with cross-flaws using rock bolt," *Tunnelling and Underground Space Technology*, vol. 51, pp. 346–353, 2016.

[11] D. Deb and K. C. Das, "Modelling of fully grouted rock bolt based on enriched finite element method," *International Journal of Rock Mechanics and Mining Sciences*, vol. 48, no. 2, pp. 283–293, 2011.

[12] Y. H. Hatzor, X.-T. Feng, S. Li, G. Yagoda-Biran, Q. Jiang, and L. Hu, "Tunnel reinforcement in columnar jointed basalts: the role of rock mass anisotropy," *Tunnelling and Underground Space Technology*, vol. 46, pp. 1–11, 2015.

[13] L. He and Q. B. Zhang, "Numerical investigation of arching mechanism to underground excavation in jointed rock mass," *Tunnelling and Underground Space Technology*, vol. 50, pp. 54–67, 2015.

[14] P. Jia and C. A. Tang, "Numerical study on failure mechanism of tunnel in jointed rock mass," *Tunnelling and Underground Space Technology*, vol. 23, no. 5, pp. 500–507, 2008.

[15] S. Maghous, D. Bernaud, and E. Couto, "Three-dimensional numerical simulation of rock deformation in bolt-supported tunnels: a homogenization approach," *Tunnelling and Underground Space Technology*, vol. 31, no. 5, pp. 68–79, 2012.

[16] J. Nemcik, S. Ma, N. Aziz, T. Ren, and X. Geng, "Numerical modelling of failure propagation in fully grouted rock bolts subjected to tensile load," *International Journal of Rock Mechanics and Mining Sciences*, vol. 71, pp. 293–300, 2014.

[17] J. Shang, Y. Yokota, Z. Zhao, and W. Dang, "DEM simulation of mortar-bolt interface behaviour subjected to shearing," *Construction and Building Materials*, vol. 185, pp. 120–137, 2018.

[18] Y. Cai, T. Esaki, and Y. Jiang, "A rock bolt and rock mass interaction model," *International Journal of Rock Mechanics and Mining Sciences*, vol. 41, no. 7, pp. 1055–1067, 2004.

[19] C. Cao, T. Ren, C. Cook, and Y. Cao, "Analytical approach in optimising selection of rebar bolts in preventing rock bolting failure," *International Journal of Rock Mechanics and Mining Sciences*, vol. 72, pp. 16–25, 2014.

[20] M. Ghadimi, K. Shahriar, and H. Jalalifar, "A new analytical solution for the displacement of fully grouted rock bolt in rock joints and experimental and numerical verifications," *Tunnelling and Underground Space Technology*, vol. 50, pp. 143–151, 2015.

[21] J. Liu, H. Yang, H. Wen, and X. Zhou, "Analytical model for the load transmission law of rock bolt subjected to open and sliding joint displacements," *International Journal of Rock Mechanics and Mining Sciences*, vol. 100, pp. 1–9, 2017.

[22] S. Ma, J. Nemcik, N. Aziz, and Z. Zhang, "Analytical model for rock bolts reaching free end slip," *Construction and Building Materials*, vol. 57, pp. 30–37, 2014.

[23] C. H. Tan, "Difference solution of passive bolts reinforcement around a circular opening in elastoplastic rock mass," *International Journal of Rock Mechanics and Mining Sciences*, vol. 81, pp. 28–38, 2016.

[24] B. Duan, H. Xia, and X. Yang, "Impacts of bench blasting vibration on the stability of the surrounding rock masses of roadways," *Tunnelling and Underground Space Technology*, vol. 71, pp. 605–622, 2018.

[25] M. He, W. Gong, J. Wang et al., "Development of a novel energy-absorbing bolt with extraordinarily large elongation and constant resistance," *International Journal of Rock Mechanics and Mining Sciences*, vol. 67, pp. 29–42, 2014.

[26] W. Wang, Q. Song, C. Xu, and H. Gong, "Mechanical behaviour of fully grouted GFRP rock bolts under the joint action of pre-tension load and blast dynamic load," *Tunnelling and Underground Space Technology*, vol. 73, pp. 82–91, 2018.

[27] X. Wu, Y. Jiang, Z. Guan, and G. Wang, "Estimating the support effect of energy-absorbing rock bolts based on the mechanical work transfer ability," *International Journal of Rock Mechanics and Mining Sciences*, vol. 103, pp. 168–178, 2018.

[28] F. D. Patton, "Multiple modes of shear failure in rock," in *Proceedings of 1st ISRM Congress*, pp. 711–721, Lisbon, Portugal, September-October 1966.

[29] A. L. LeRoy and G. Peter, "Mechanics of bond and slip of deformed bars in concrete," *ACI Journal Proceedings*, vol. 64, no. 11, pp. 711–721, 1967.